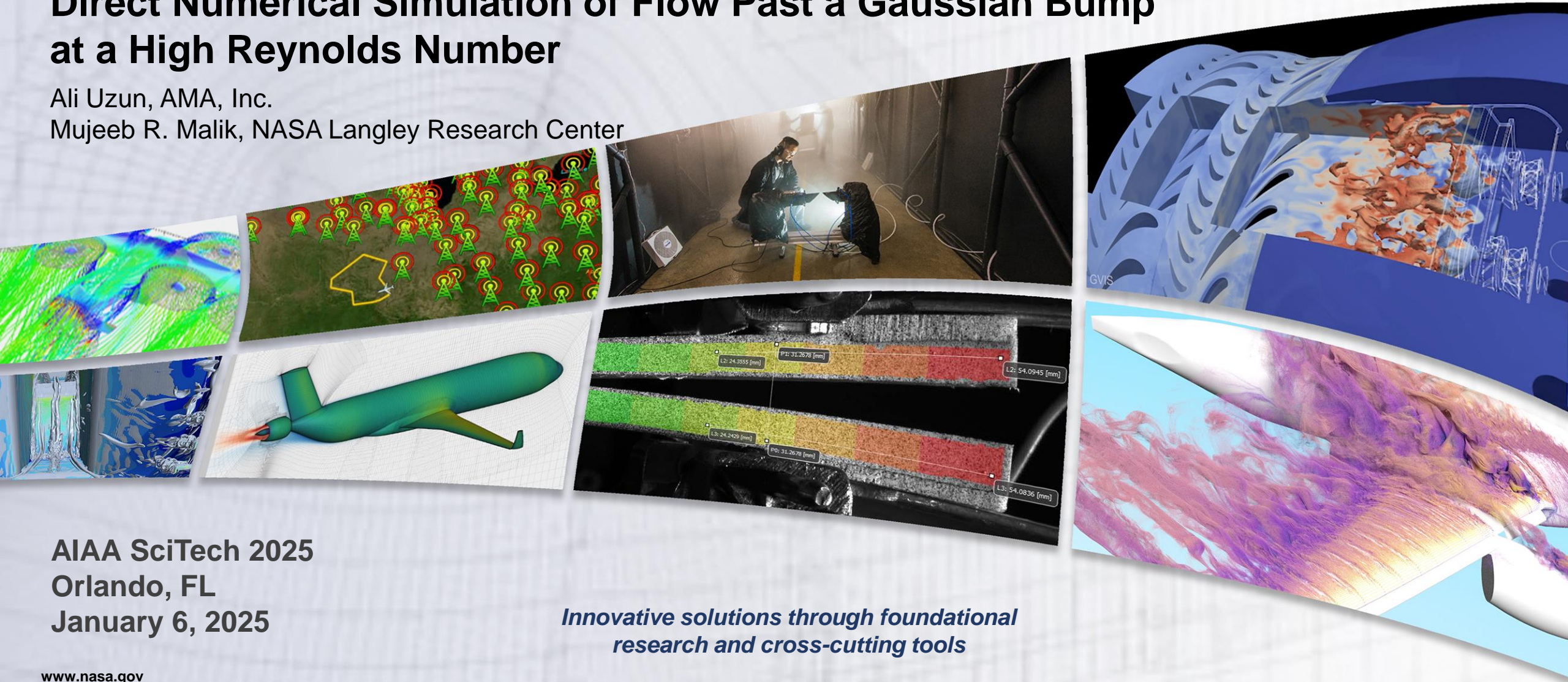


Transformational Tools and Technologies (T<sup>3</sup>) Project

# Direct Numerical Simulation of Flow Past a Gaussian Bump at a High Reynolds Number

Ali Uzun, AMA, Inc.

Mujeeb R. Malik, NASA Langley Research Center

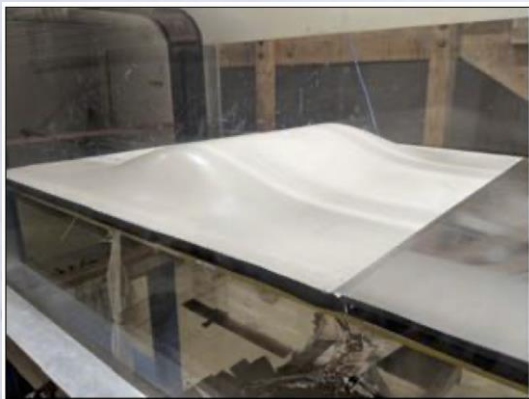


AIAA SciTech 2025  
Orlando, FL  
January 6, 2025

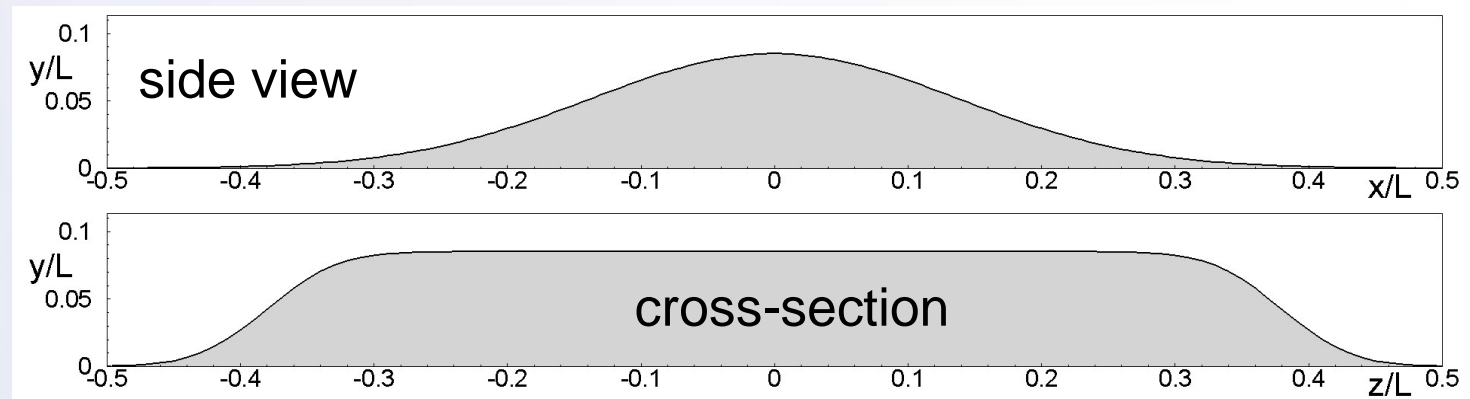
*Innovative solutions through foundational  
research and cross-cutting tools*

# Introduction

- **The objective is to provide DNS data for turbulent flow subjected to pressure gradients**
  - Both favorable and adverse, where the latter leads to flow separation
- **Inspired by an experiment over a canonical flow configuration: “Boeing Speed Bump”**
  - Experiment was sponsored by 4 US Government Agencies and Boeing
  - Experiment was conducted at University of Notre Dame, and reported by Gray et al. (2021-2023)
    - Experimental data available at NASA TMR
- **DNS is for a simplified bump, as DNS is prohibitively expensive for the 3D bump**
  - Spanwise-periodic, ignoring the effects of bump shoulders, tunnel side walls and top wall
    - Therefore, we don't necessarily expect agreement with the experiment



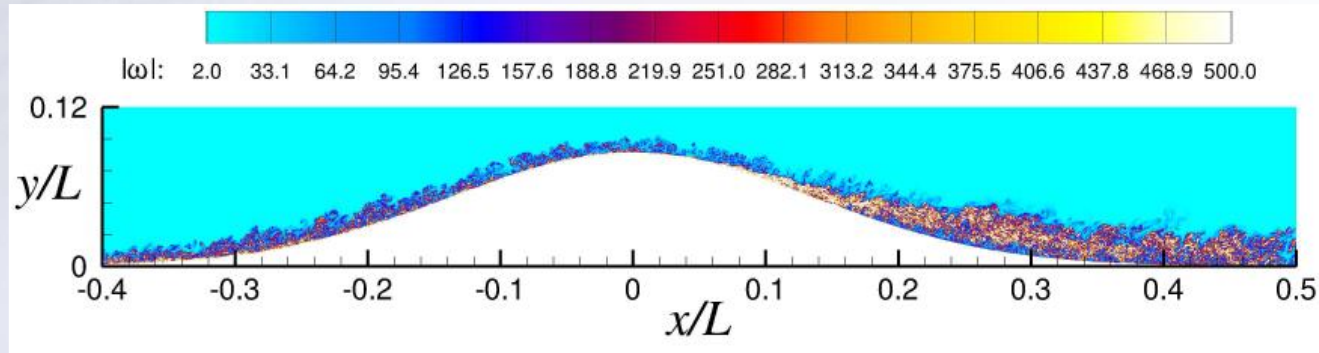
3-D geometry in tunnel



$L$  is the length & span, side walls at:  $z/L = \pm 0.5$ , ceiling at:  $y/L = 0.5$

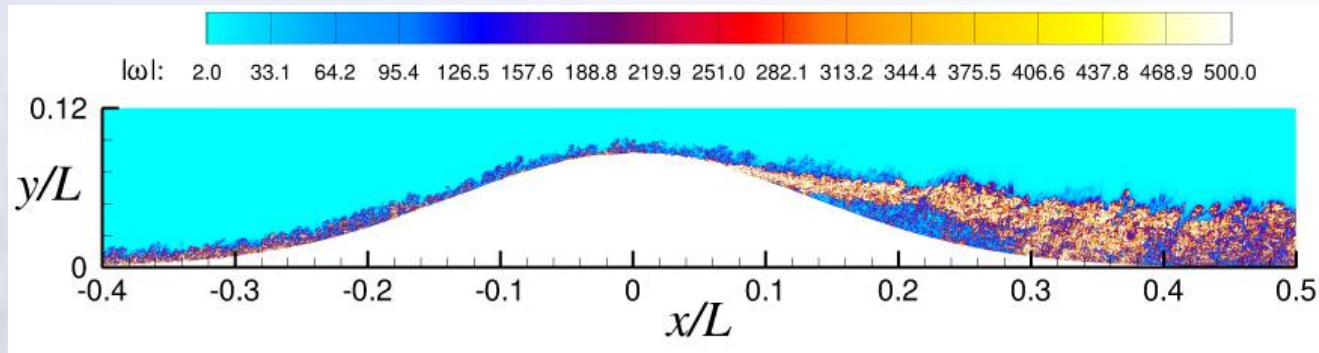
# Spanwise-Periodic DNS of the Speed Bump Flow

- We have previously performed spanwise-periodic DNS of the speed-bump flow at two different Reynolds numbers:  $Re_L = \rho_\infty U_\infty L / \mu_\infty = 1$  and 2 million
  - DNS data are available at NASA TMR



(a)  $Re_L = 1$  million

Incipient separation



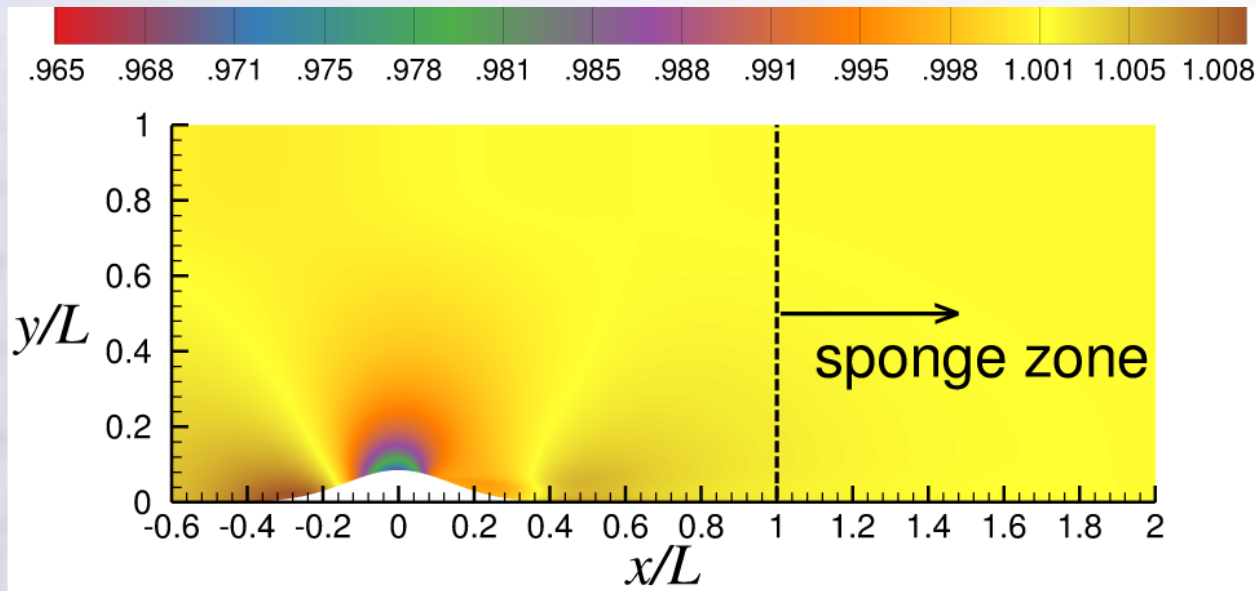
(b)  $Re_L = 2$  million

Strong separation

- The current DNS is at  $Re_L = 4$  million, the highest Reynolds number of the experiment
  - Enabled by the compute time available through the SummitPLUS program of ORNL

# Computational Domain/Schematic for $Re_L = 4$ Million Simulation

- Spanwise-periodic configuration with span of  $0.08L$  (same as in  $Re_L = 2$  million case)
- Freestream Mach number is set to 0.2 (same as in  $Re_L = 2$  million case)
  - Same Mach number as in the experiment
- Mean inflow profile taken from RANS, inflow boundary-layer  $Re_\theta \approx 3314$
- Turbulent inflow generation based on the recycling-rescaling method (see paper for Ref.)
- Viscous isothermal boundary condition on lower wall
- Nonreflecting boundary condition at  $y/L = 1$  (same as in  $Re_L = 2$  million case)
  - Experiment had a solid top wall at  $y/L = 0.5$
- Sponge zone with characteristic boundary condition on outflow boundary

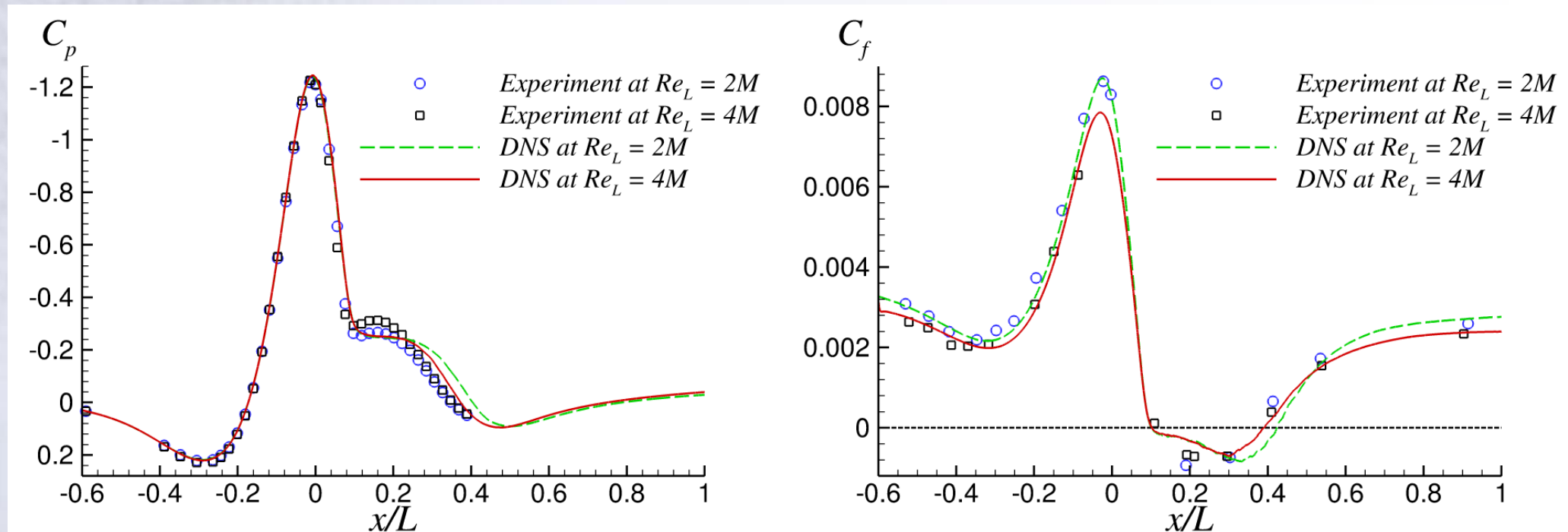


Contours denote the mean pressure normalized by a reference value

# Simulation Details

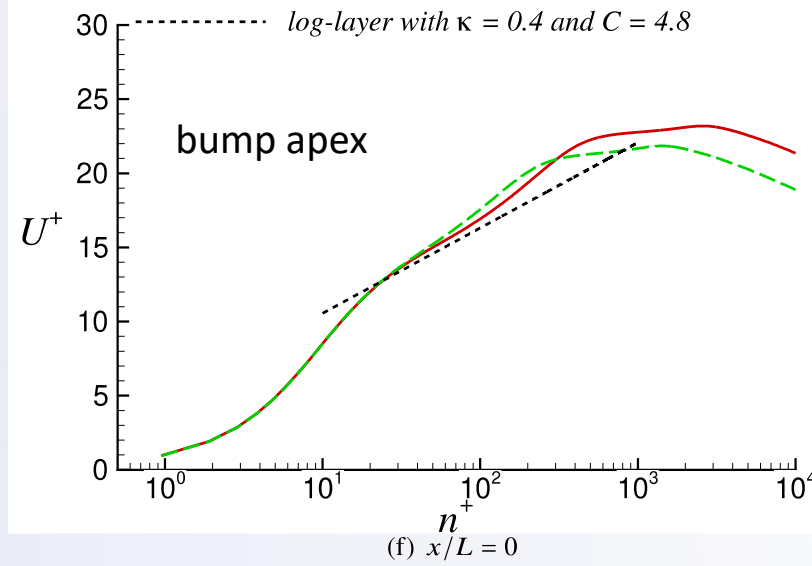
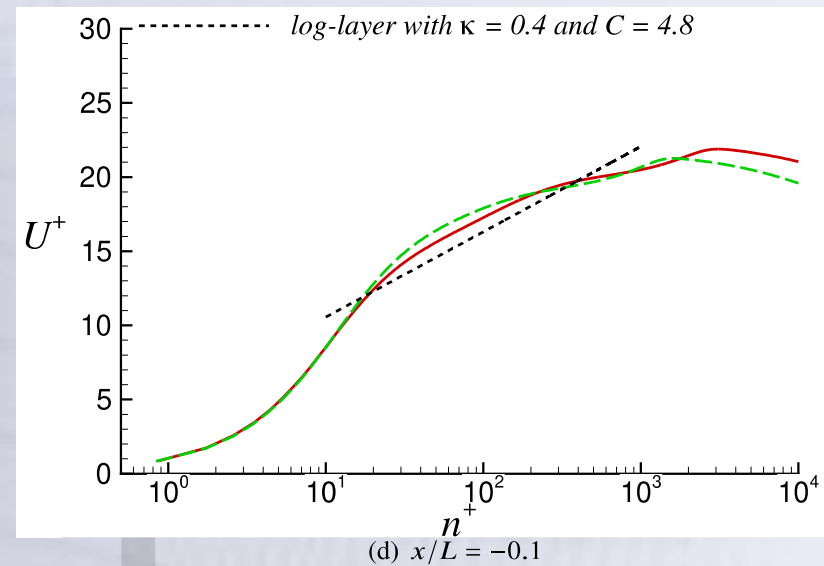
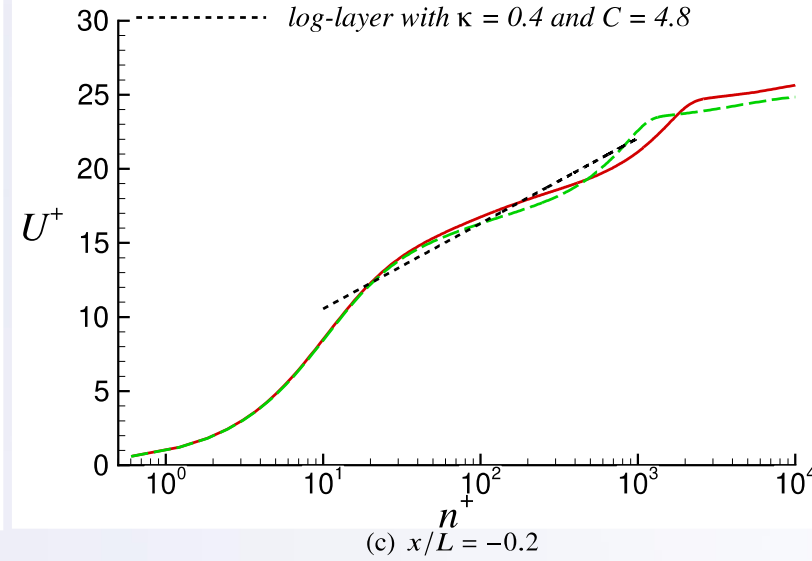
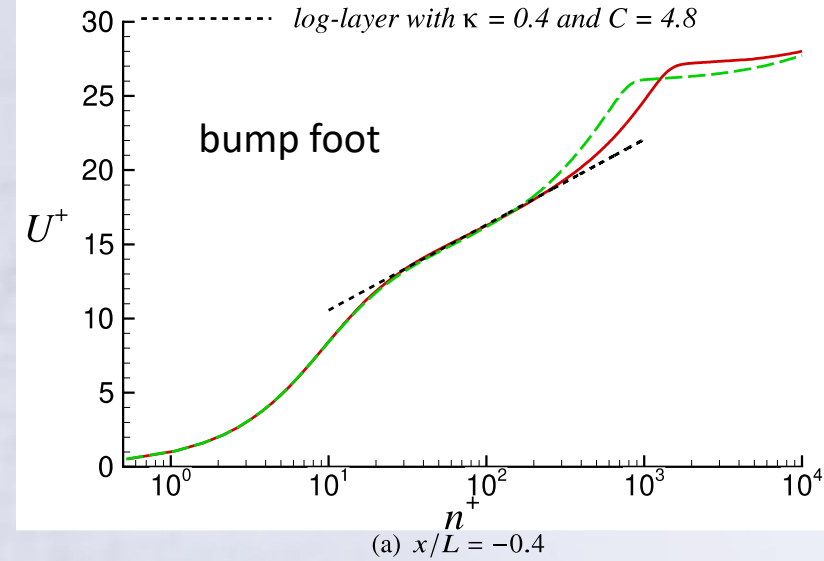
- About 48 billion grid points total ( $N(x,y,z) = 23040 \times 672 \times 3072$ )
- Flow solver for graphics processing units (GPUs) :
  - Compressible Navier-Stokes equations in generalized curvilinear coordinates
  - Optimized explicit 4<sup>th</sup>-order finite-difference with 6<sup>th</sup>-order filtering scheme
  - 3<sup>rd</sup>-order, three-stage, explicit Runge-Kutta time integration scheme
- DNS initial conditions are generated by a hybrid RANS-LES on a much coarser grid
- 1.4 million time steps to compute one convective time unit ( $L/U_\infty$ )
- 2160 NVIDIA V100 GPUs to perform the DNS on Summit at ORNL
- About 80 hours of wall-clock time per  $L/U_\infty$
- Flow statistics gathered over 16  $L/U_\infty$  (10 domain flow-through times) are averaged in time and along the span
- Mean velocity and turbulence stress components computed in the Cartesian coordinate system are transformed to the local orthogonal coordinate system at a given location on the bump surface using the local wall-normal and surface tangent vectors

# Surface Pressure and Skin-Friction Distribution Comparisons



- Both DNS results show good agreement with experiments upstream of separation
- Differences in separated region are due to stronger reversed flow in the experiments
  - Effect of 3-dimensionality (bump shoulders and tunnel side walls) not modeled in DNS
- Despite a nearly identical separation point, the higher  $Re_L$  DNS has earlier reattachment relative to the lower  $Re_L$  case, due to the faster shear layer growth in the higher  $Re_L$  case

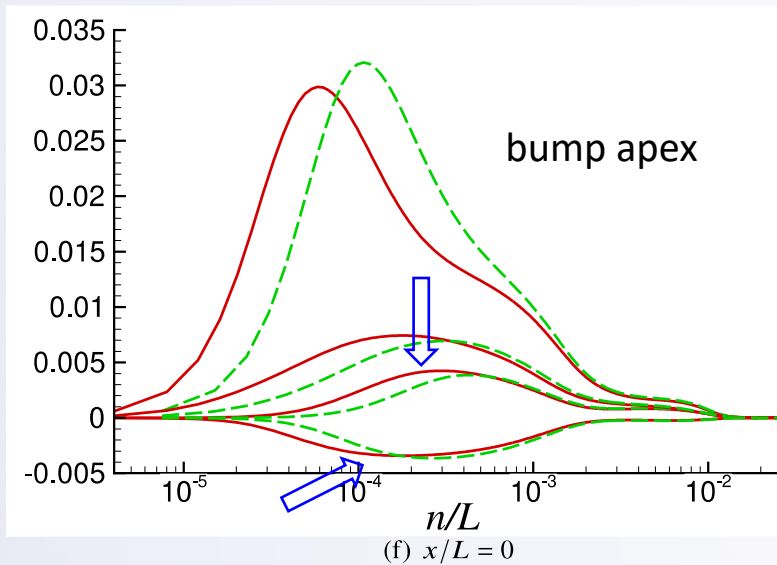
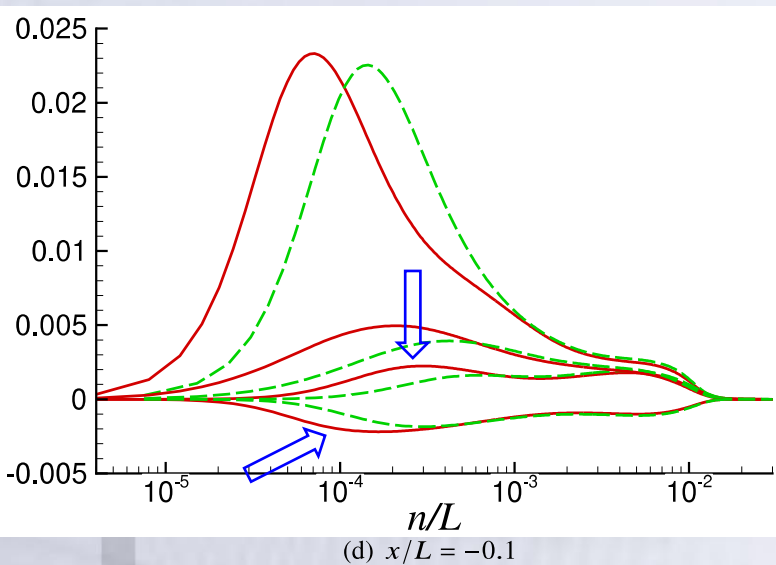
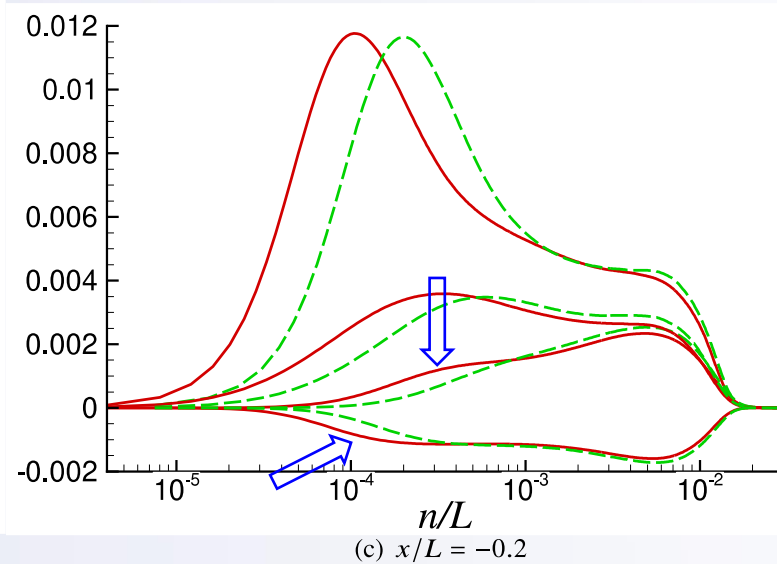
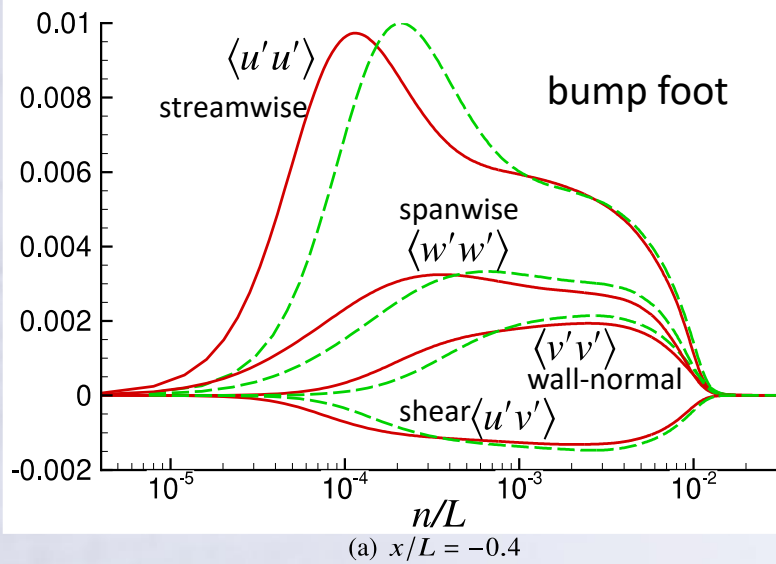
# Streamwise Velocity Profiles in Wall Units over Windward Side



- Flow passes through mild adverse pressure gradient over concave curvature before reaching bump foot
- At the bump foot, log-layer intercept constant is lower than the typical range expected for a zero pressure-gradient boundary layer; log-layer is broader in the higher  $Re_L$  flow
- Acceleration over the curved surface significantly alters the profile shapes
- Log-layers shift upward in addition to other profile changes occurring in the outer region
- The log-layer of the lower  $Re_L$  flow experiences a greater upward shift
- Strong adverse-pressure gradient effect starting ahead of apex leads to a downward shift in the log-layers and other profile changes in outer region

Solid red line:  $Re_L = 4$  million, Dashed green line:  $Re_L = 2$  million

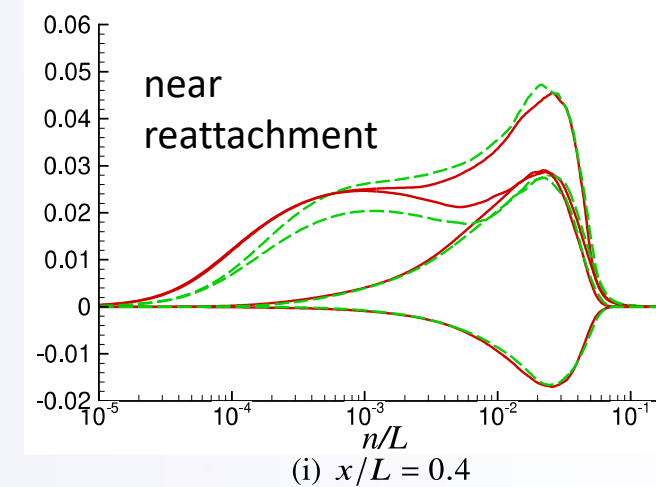
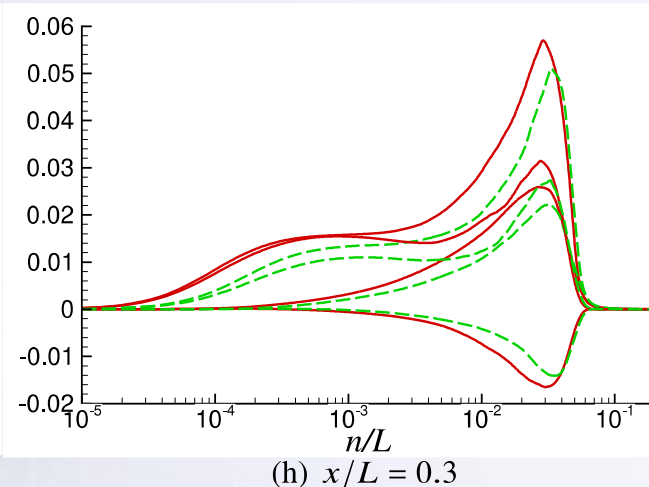
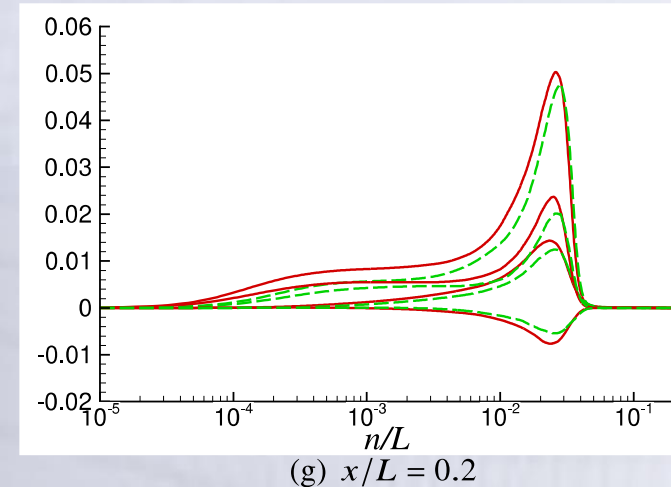
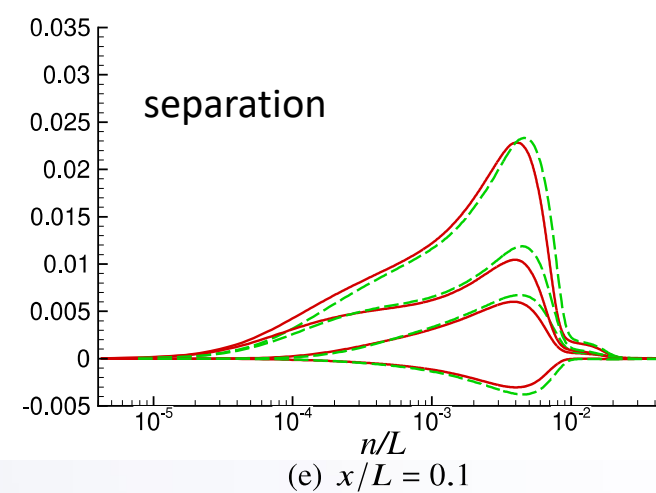
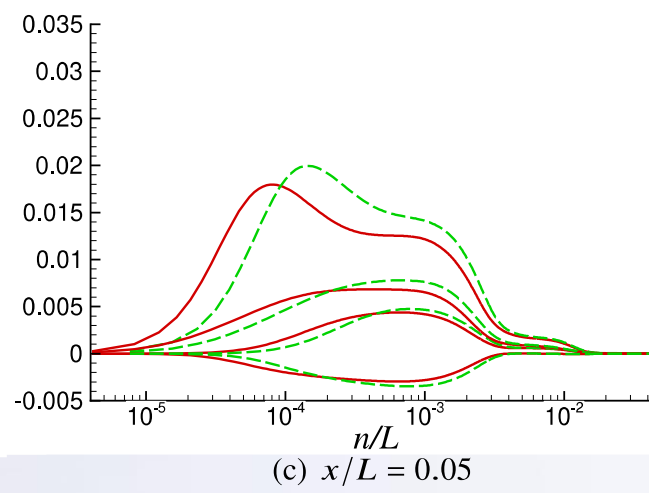
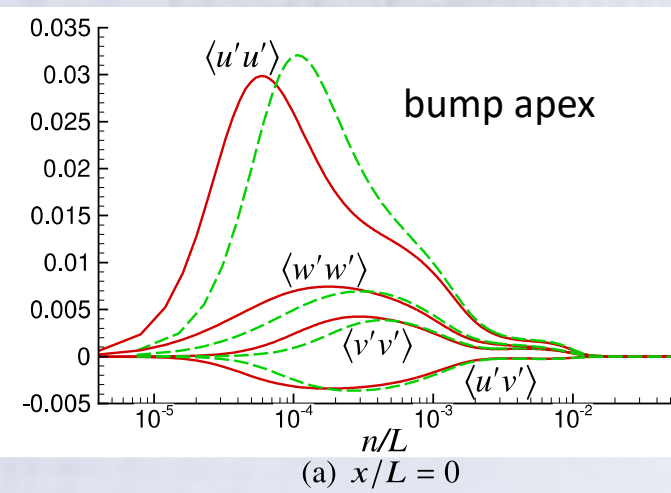
# Reynolds Stress Profiles in Outer Units over Windward Side



- Original near-wall peaks of the streamwise and spanwise components strengthen as the flow accelerates
- New near-wall peaks emerge in the wall-normal and shear components, as indicated by the blue arrows, while their original outer peaks weaken deep into the acceleration region
- Emergence of new near-wall peaks happens faster in the higher  $Re_L$  flow
- Formation of near-wall peaks in the wall-normal and shear components in parallel with the strengthening peaks of the other two components indicates generation of an internal layer beneath the accelerated boundary layer
- The respective peak of each stress component is closer to the wall in the higher  $Re_L$  flow

Solid red line:  $Re_L = 4$  million, Dashed green line:  $Re_L = 2$  million

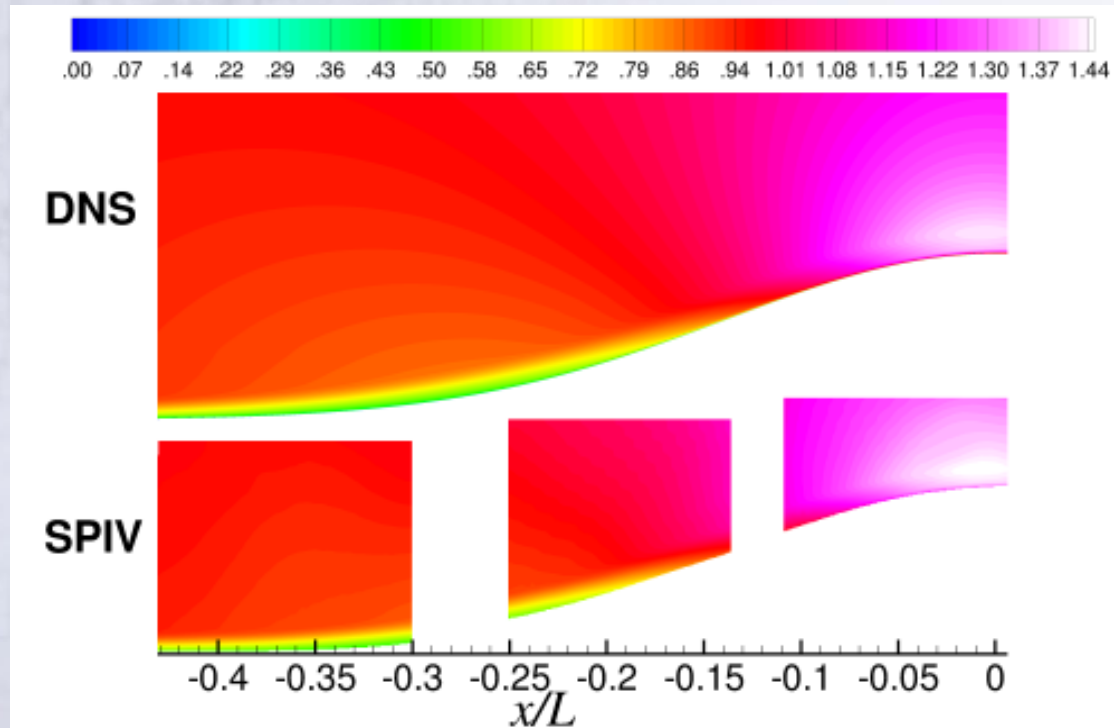
# Reynolds Stress Profiles in Outer Units over Leeward Side



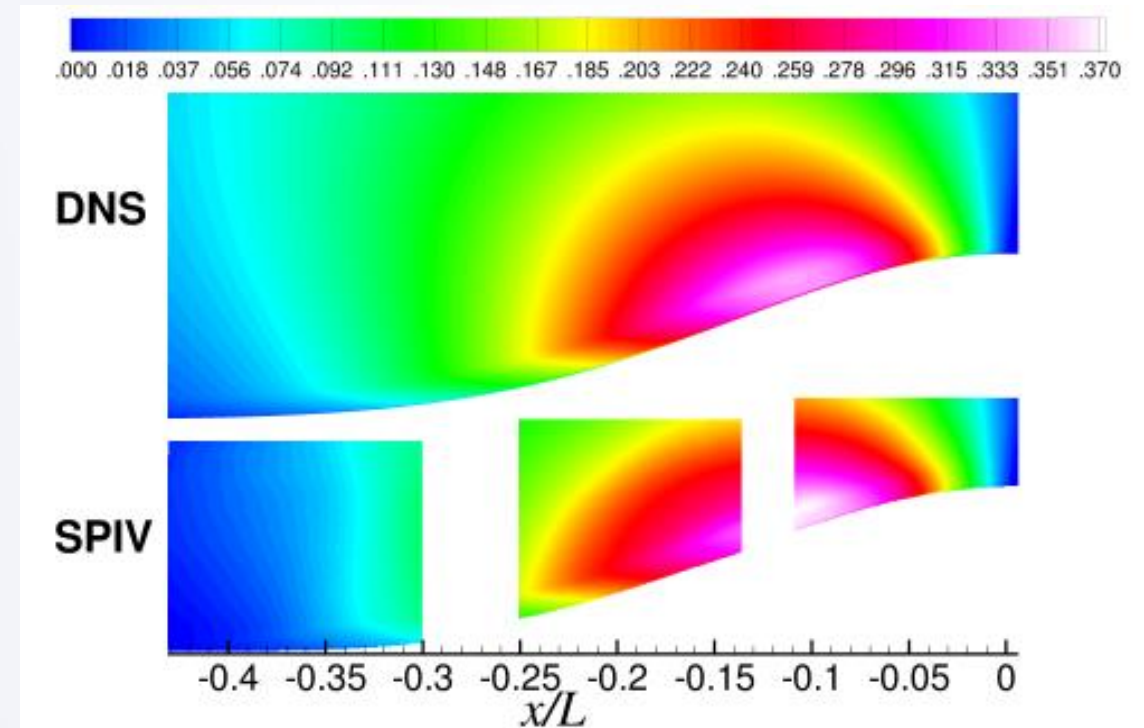
Solid red line:  $Re_L = 4$  million, Dashed green line:  $Re_L = 2$  million

- At separation, larger peak stress values in the lower  $Re_L$  flow
- Differences in the initial state will have implications in shear layer development further downstream
- In the separated shear layer, larger peak stress values of the higher  $Re_L$  flow indicate more energetic structures and faster shear layer growth
- Faster growth of the higher  $Re_L$  shear layer correlates with earlier reattachment

# Mean Velocity Comparisons with Experiment for $Re_L = 4$ Million



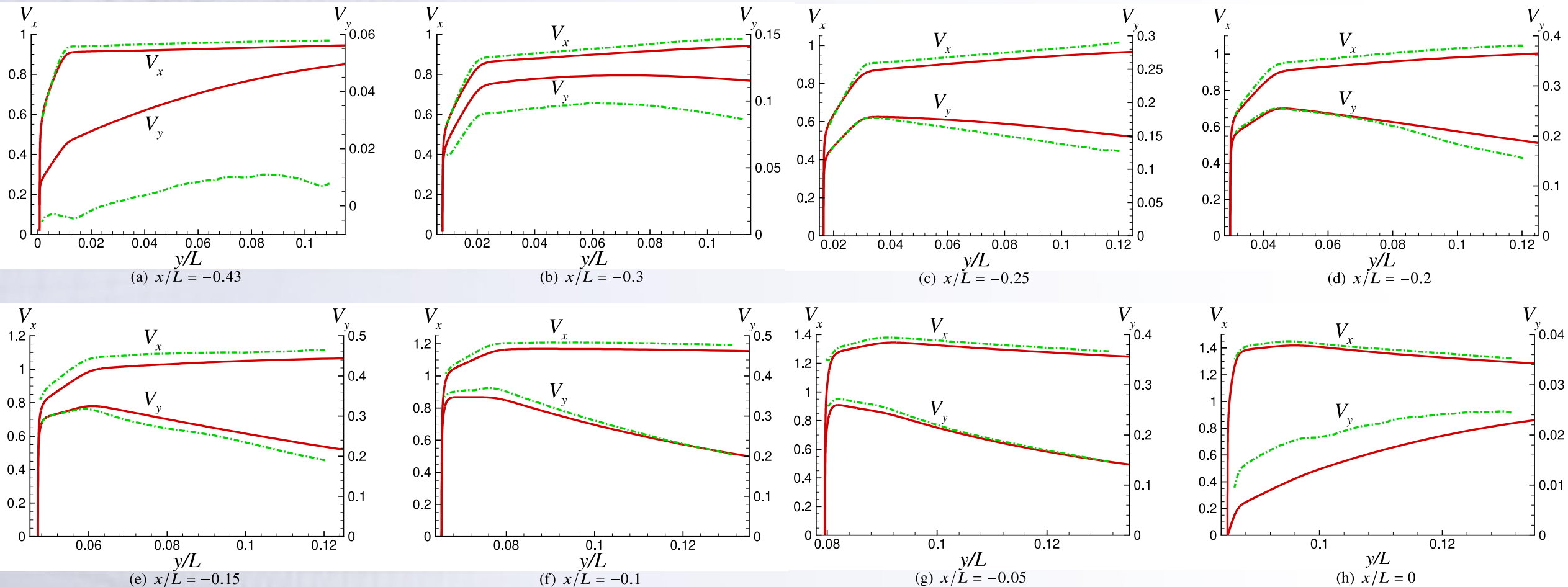
(a) Mean velocity component in the x direction,  $V_x$



(b) Mean velocity component in the y direction,  $V_y$

- Mean velocity components are defined in the Cartesian coordinate system
- Reasonable overall agreement between DNS and SPIV over the windward side of bump
- Some differences exist, likely due to the tunnel blockage effect in the experiment
- Velocity profile comparisons at several  $x/L$  are examined next

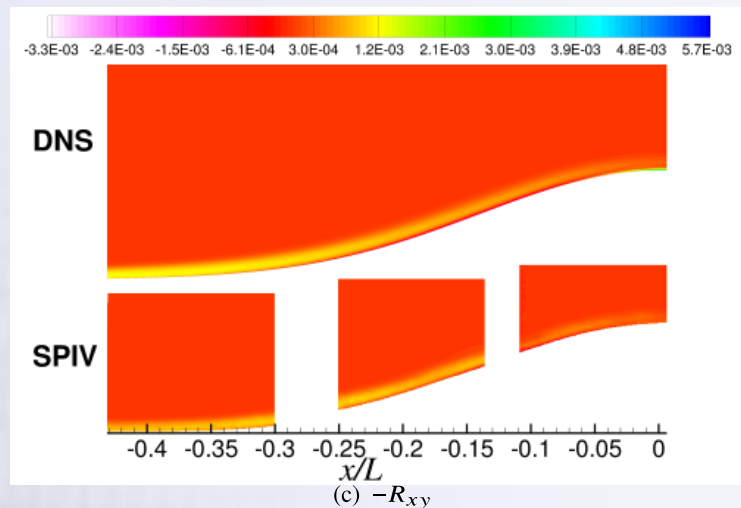
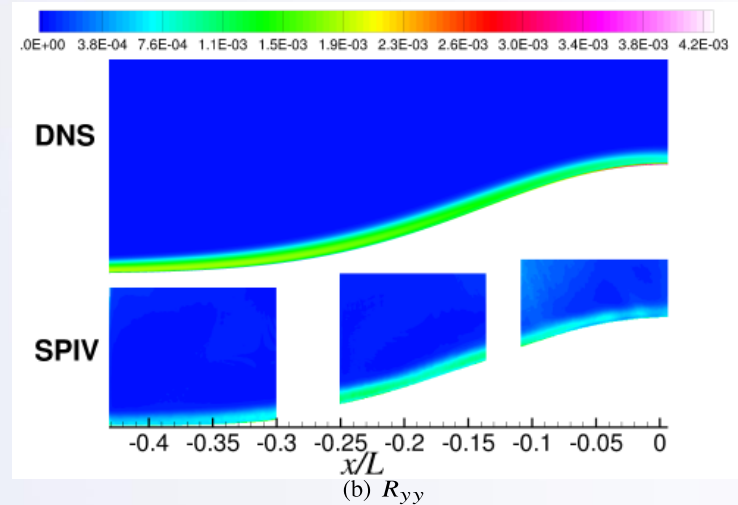
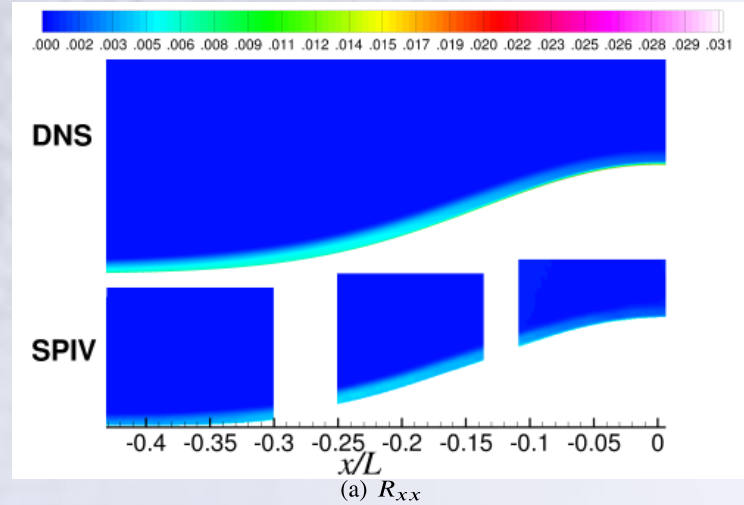
# Velocity Profile Comparisons with SPIV for $Re_L = 4$ Million



**Solid red line: DNS, Dash-dotted green line: Experiment**

- **Note: Vertical scales (particularly for  $V_y$ ) are different in each plot**
  - **Where differences are large for vertical velocity, magnitude is relatively small**

# Reynolds Stress Component Comparisons for $Re_L = 4$ Million



□ Reynolds stress components are defined in the Cartesian coordinate system:

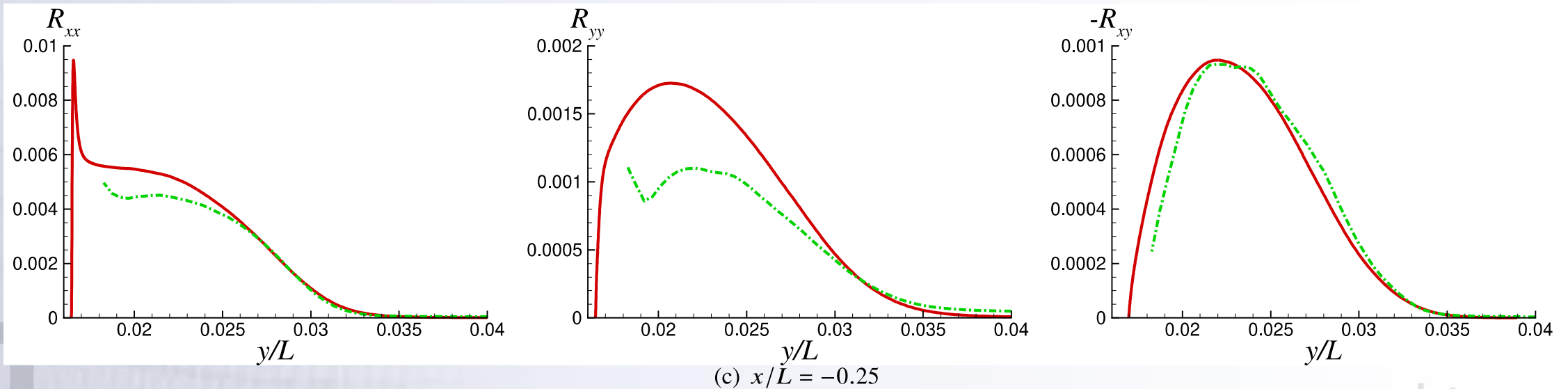
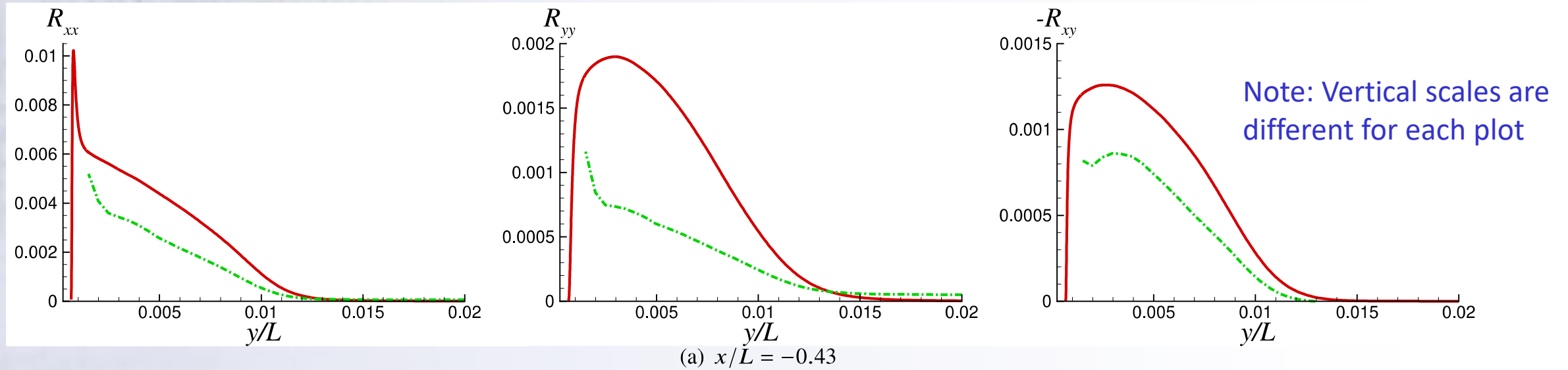
$$R_{xx} = \text{axial component}$$

$$R_{yy} = \text{vertical component}$$

$$R_{xy} = \text{shear component}$$

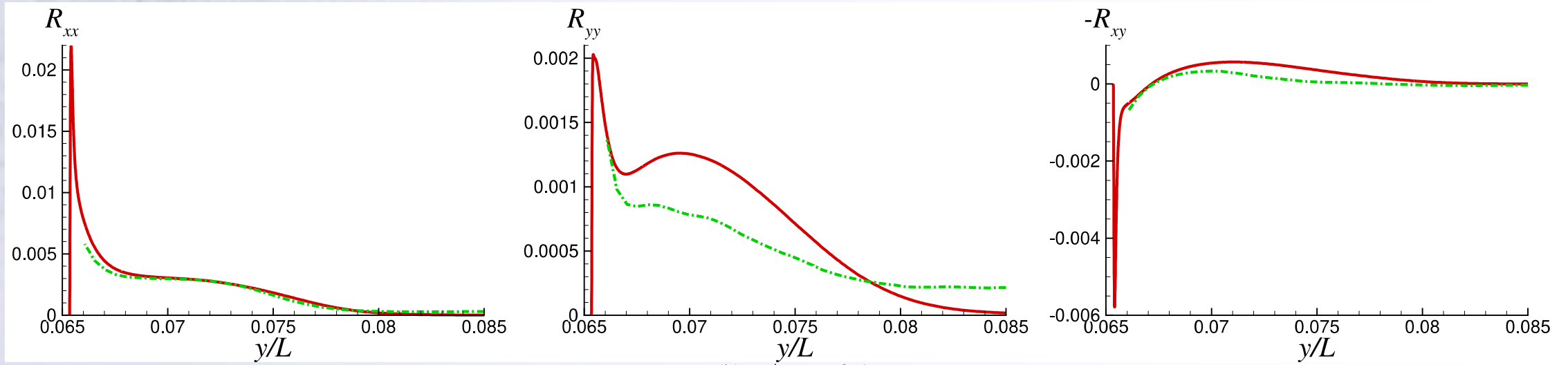
- More significant differences exist in the Reynolds stress component comparisons
- Reynolds stress profile comparisons at several  $x/L$  are examined next

# Reynolds Stress Profile Comparisons with SPIV for $Re_L = 4$ Million

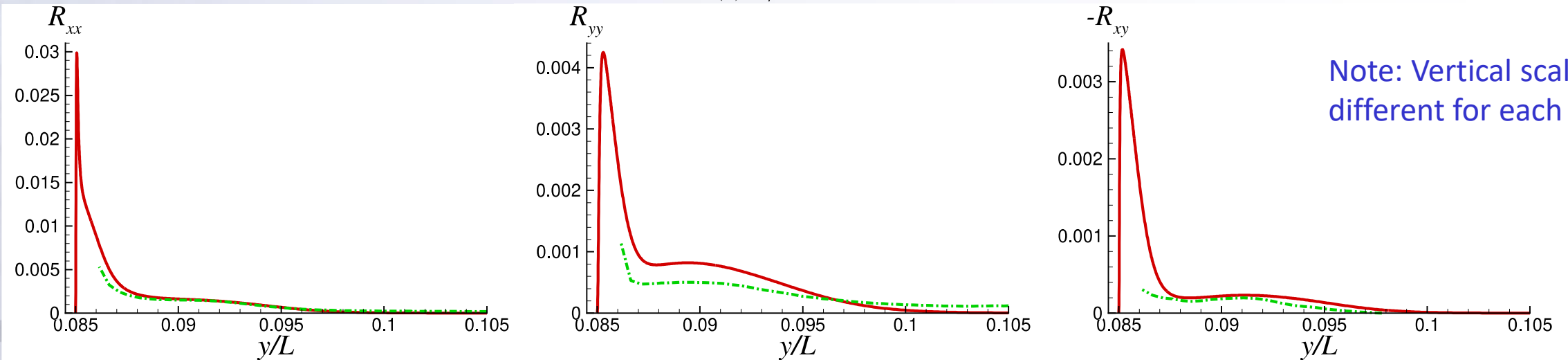


Solid red line: DNS, Dash-dotted green line: Experiment

# Reynolds Stress Profile Comparisons with SPIV for $Re_L = 4$ Million



(b)  $x/L = -0.1$



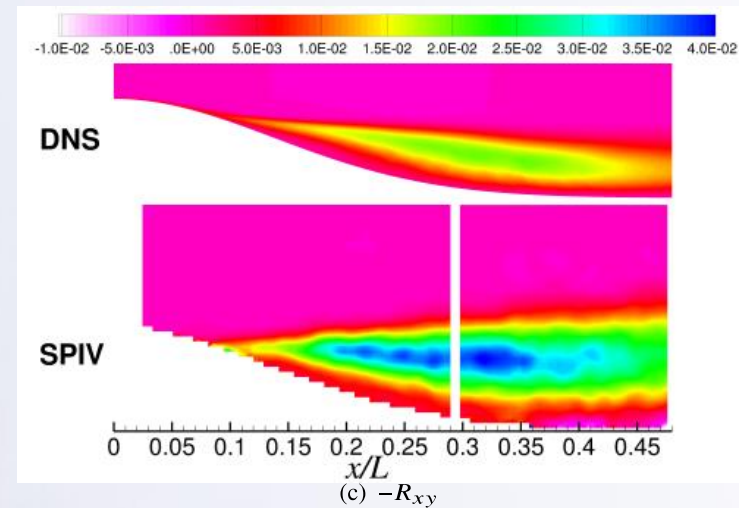
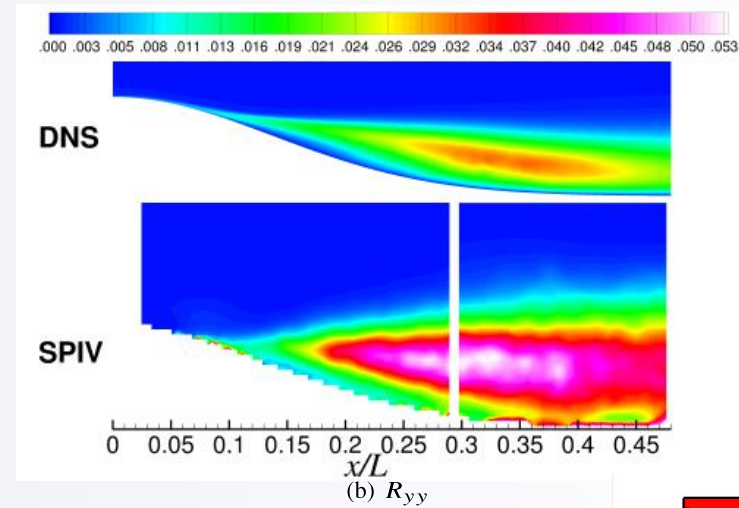
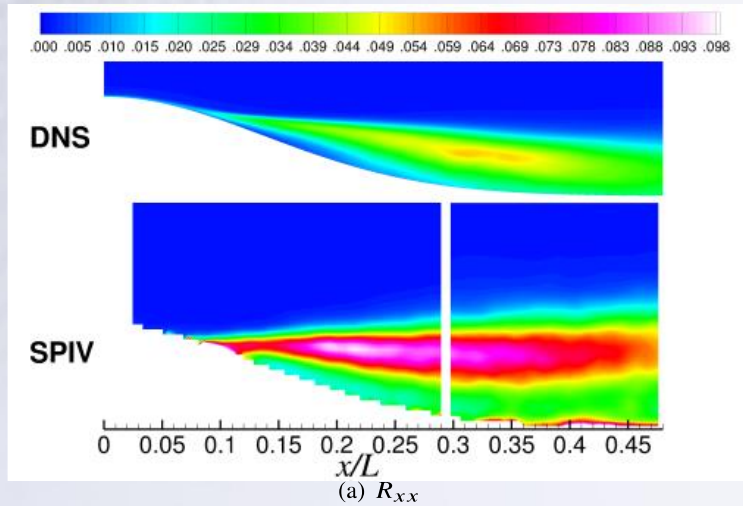
Note: Vertical scales are different for each plot

(d)  $x/L = 0$

Solid red line: DNS, Dash-dotted green line: Experiment

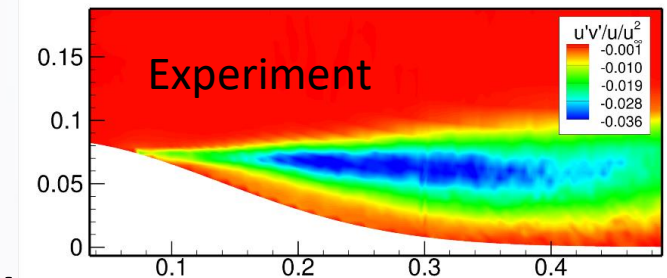
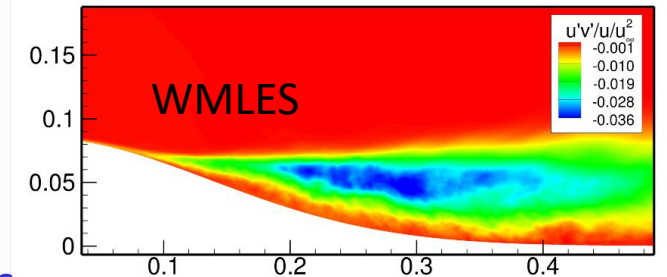
# Leeward Side Reynolds Stress Components for $Re_L = 4$ Million

## Results along the bump centerline



Shear stress

Iyer & Malik, AIAA Paper 2023-0253: 3D effects included



- Very significant differences are present in the Reynolds stress components
- Peak stress values of the experiment are nearly double of the respective DNS values
  - Effects of 3D setup of the experiment, not modeled in the DNS

# Summary and Concluding Remarks

- **The comparisons between our  $Re_L = 4$  and 2 million simulations reveal that:**
  - Both cases experience flow separation at nearly the same location shortly past the bump apex
  - The separated shear layer has a faster growth rate and earlier reattachment in the higher  $Re_L$  flow
- **On the windward side**
  - Very good agreement with experiment in  $C_p$  and  $C_f$  distributions upstream of separation for both  $Re_L$  cases
  - Reasonable agreement with experiment in velocity components
  - Less satisfactory agreement with experiment for Reynolds stresses
- **On the leeward side**
  - Major differences in mean shear layer orientation and turbulence stress levels, due to effects of 3D experimental setup, not modeled in DNS
- **DNS provides data for assessment/improvement of lower fidelity models**
  - Data will be uploaded to NASA TMR
  - Data also collected for turbulence budgets and pressure-strain correlation, yet to be analyzed

# Acknowledgments

- This research is sponsored by the NASA Transformational Tools and Technologies Project of the Transformative Aeronautics Concepts Program under the Aeronautics Research Mission Directorate
- This work also used the now-decommissioned Summit system of the Oak Ridge Leadership Computing Facility at the Oak Ridge National Laboratory, which is supported by the Office of Science of the U.S. Department of Energy under Contract No. DE-AC05-00OR22725

